Tellus (2001), 53B, 133–149
Printed in UK. All rights reserved

TELLUS
ISSN 0280–6509

Kinetic limitations on cloud droplet formation and impact on cloud albedo

By ATHANASIOS NENES[1], STEVEN GHAN[2], HAYDER ABDUL-RAZZAK[3], PATRICK Y. CHUANG[4] and JOHN H. SEINFELD[1]*, [1]*Department of Chemical Engineering, Mail Code 210-41, California Institute of Technology, Pasadena, California, 91125, USA;* [2]*Pacific Northwest National Laboratory, Richland, Washington, 99352, USA;* [3]*Texas A&M University-Kingsville, Kingsville, Texas, 78363, USA;* [4]*NCAR, Boulder, Colorado, 80307, USA*

(Manuscript received 3 February 2000; in final form 2 October 2000)

ABSTRACT

Under certain conditions mass transfer limitations on the growth of cloud condensation nuclei (CCN) may have a significant impact on the number of droplets that can form in a cloud. The assumption that particles remain in equilibrium until activated may therefore not always be appropriate for aerosol populations existing in the atmosphere. This work identifies three mechanisms that lead to kinetic limitations, the effect of which on activated cloud droplet number and cloud albedo is assessed using a one-dimensional cloud parcel model with detailed microphysics for a variety of aerosol size distributions and updraft velocities. In assessing the effect of kinetic limitations, we have assumed as cloud droplets not only those that are strictly activated (as dictated by classical Köhler theory), but also unactivated drops large enough to have an impact on cloud optical properties. Aerosol number concentration is found to be the key parameter that controls the significance of kinetic effects. Simulations indicate that the equilibrium assumption leads to an overprediction of droplet number by less than 10% for marine aerosol; this overprediction can exceed 40% for urban type aerosol. Overall, the effect of kinetic limitations on cloud albedo can be considered important when equilibrium activation theory consistently overpredicts droplet number by more than 10%. The maximum change in cloud albedo as a result of kinetic limitations is less than 0.005 for cases such as marine aerosol; however albedo differences can exceed 0.1 under more polluted conditions. Kinetic limitations are thus not expected to be climatically significant on a global scale, but can regionally have a large impact on cloud albedo.

1. Introduction

Much of the uncertainty associated with quantifying the indirect climatic effect of aerosols originates in the complex relationship between aerosols and cloud droplets. Approximate analytical expressions that predict those aerosol particles that activate to form cloud droplets have been proposed for implementation in general circulation models (GCMs) (Ghan et al., 1993; Liu and Wang, 1996; Abdul-Razzak et al., 1998). These parameterizations generally rely on the assumption that particles are at equilibrium with the ambient (supersaturated) water vapor concentration until activated as cloud condensation nuclei (CCN). The number of droplets formed in a cloud can therefore be estimated from the number of CCN active at the maximum supersaturation in the cloud updraft. The problem of droplet nucleation parameterization is then reduced to the

* Corresponding author.
email: seinfeld@its.caltech.edu

problem of determining the maximum supersaturation in the cloud parcel.

The assumption that all particles respond instantaneously to any changes in supersaturation leads to a problem: the amount of water absorbed by the largest aerosol particles when they activate can be larger than the amount of water vapor available in the cloud parcel. This problem, known for a long time, is not serious when predicting the number of droplets, because although not activated, these particles have an equilibrium saturation ratio very close to unity, as activated particles do. As a consequence, their growth can be parameterized as if they were activated. In addition, the number of large particles that give rise to this problem are usually negligible compared to the concentration of smaller particles of the distribution, so the errors in cloud droplet number overall are expected to be small.

The assumption of equilibrium, however, can lead to a discrepancy in droplet number as a result of mass transfer limitations. Chuang et al. (1997) have shown that under certain circumstances growth kinetics may retard the growth of CCN sufficiently to limit the number of activated droplets formed. By comparing the time scale for particle growth at equilibrium with that for actual condensational growth, Chuang et al. (1997) conclude that particles with critical supersaturation less than a threshold value do not have time to grow larger than their critical size, and thus do not activate. This suggests that equilibrium models that diagnose droplet formation from maximum supersaturation may systematically overestimate the number of activated droplets formed. Such a systematic bias could have implications for estimates of indirect aerosol radiative forcing of climate. It is difficult, however, to draw firm conclusions simply from a comparison of timescales because growth kinetics depend on the full time history of supersaturation and particle growth. Furthermore, the timescales controlling the growth of the droplets change drastically as the populations grows. A more conclusive method of evaluating the importance of growth kinetics is obtained by explicitly simulating the kinetic growth process and then comparing the simulated number of droplets formed with that predicted by equilibrium theory for the same CCN concentration and maximum supersaturation.

Furthermore, it is incorrect to consider cloud drops as only those that are strictly activated (as defined by Köhler theory); the presence of large unactivated droplets cannot be neglected. This issue becomes even more important when slightly soluble substances are present in the aerosol (Laaksonen et al., 1998). The condensational growth of an aerosol population prescribes that particles with very large dry diameters, although not activated, lead to roughly the same size of activated droplets and thus belong to the cloud droplet population. With this in mind, one can define as CCN all particles that produce droplets that are larger than the smallest particle that is strictly activated. This cloud droplet definition differs slightly from that given by Pandis et al. (1990); we do not consider as droplets all the particles that exceed their critical diameter or have a critical supersaturation lower than ambient supersaturation, but only those comparable in size to those that are strictly activated.

Based on the previous discussion, the inertial mechanism of Chuang et al. (1997) is believed not to contribute to any bias in the predicted droplet number when the equilibrium assumption is invoked. However, there are other kinetic limitation mechanisms that produce particles that are much smaller than activated drops; in this sense, these mechanisms act to decrease the number of cloud droplets from that predicted strictly on the basis of equilibrium activation. This study will focus mainly on these mechanisms.

In the sections that follow, the mechanisms that lead to kinetic limitations in cloud droplet formation are presented. The models used for evaluating kinetic effects are then described, together with the relevant criteria used for assessing the potential climatic importance of these effects. Finally, simulations are presented, for a variety of updraft conditions and aerosol types, from which conclusions can be derived regarding the effect of kinetic limitations on cloud droplet number concentration and albedo.

2. Kinetic limitation mechanisms

There are three kinetic limitation processes that can inhibit the formation of cloud droplets. These mechanisms will be explained with the help of Fig. 1, which illustrates typical cloud parcel and droplet equilibrium supersaturation profiles (S and

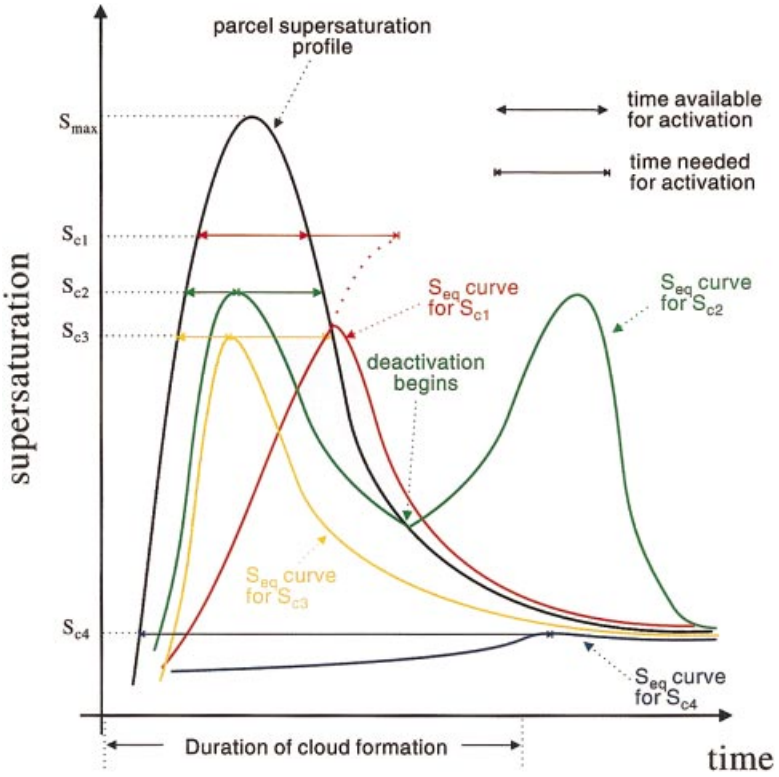

Fig. 1. Illustration of the kinetic limitation mechanisms.

S_{eq}, respectively) as a function of cloud depth, as predicted by adiabatic parcel theory. Each aerosol equilibrium curve corresponds to particles containing a different amount of solute. The equilibrium curves vary with respect to cloud depth as a consequence of droplets changing size as they traverse through the cloud column. According to equilibrium activation theory, any particle with a critical supersaturation, S_c, less than the maximum supersaturation, S_{max}, encountered in the parcel will activate. However, the time which particles are exposed to a supersaturation level is a crucial parameter; that time must be sufficiently long to allow the particle to reach its critical diameter. The droplet can be considered activated only when the wet diameter exceeds its critical value. Furthermore, to ensure constant growth of the droplet, the ambient supersaturation should be high enough for activated droplets to continuously grow throughout the duration of cloud formation.

The yellow curve of Fig. 1 represents an aerosol particle that activates and remains so throughout the entire time of cloud formation. The critical supersaturation of the particle, S_{c3}, is less than S_{max}; the time needed for activation is also less than the time during which $S \geqslant S_{c3}$. When this particle activates, its equilibrium curve will be at a maximum (with $S_{eq} = S_{c3}$); subsequently, the particle is activated and S_{eq} drops. As can be seen, the particle S_{eq} is always less than the parcel supersaturation, so the driving force for growth, $S - S_{eq}$, is always positive. This guarantees that the particle will remain activated throughout the cloud.

The same cannot be said for all the aerosol types depicted in Fig. 1. The first mechanism that limits the formation of activated droplets is the inertial mechanism described by Chuang et al. (1997). This mechanism is illustrated in Fig. 1 for the particles with a critical supersaturation S_{c4} (blue curve). These particles have a large dry diameter and a very low critical supersaturation.

The timescale of cloud formation is not sufficient for these particles to reach their critical diameter. Nonetheless, the driving force for growth is always positive, and these particles continuously grow, attaining a wet diameter similar (and actually larger) to those of the activated droplets. Thus, even though these particles do not activate, they cannot be distinguished from activated droplets, and so should be treated as such.

The red curve corresponds to a particle with a relatively high critical supersaturation, S_{c1}. The time during which $S > S_{c1}$ is not sufficient for activation. As a result, the particle initially grows, but subsequently evaporates to become an interstitial aerosol particle. This kinetic effect is the 2nd of the 3 mechanisms identified, and is termed the "evaporation mechanism". Although this is an inertial mechanism (in the sense that small particles do not respond fast enough to changes in ambient supersaturation), a different name is assigned because the particles affected behave much differently than those subject to the inertial mechanism of Chuang et al. (1997).

Finally, some particles can initially activate but become interstitial aerosol through the third mechanism, the so-called "deactivation mechanism". This is illustrated in Fig. 1 for particles of critical supersaturation S_{c2} (green curve). These particles are exposed to a supersaturation that exceeds their critical values sufficiently long to activate and do so initially. However, after a while, the parcel supersaturation drops below the droplet S_{eq}. When this happens, the growth driving force, $S - S_{eq}$, becomes negative, and these droplets begin evaporating. The rate of evaporation can be quite fast, and the droplet may deactivate and become part of the interstitial aerosol, thus decreasing the number of cloud droplets. This mechanism is not a result of mass transfer kinetic limitation, but rather a dynamic effect arising from the limited available water vapor; water transfers from activated drops to other sizes that can still grow.

The deactivation and evaporation mechanisms render the affected aerosol much smaller than the activated droplet size, leading to considerably smaller contribution to cloud optical properties. On the other hand, whereas the inertial mechanism prevents droplets from activating, it does not produce droplets that are differentiated from other activated droplets as the other two mechanisms do. When using the equilibrium assumption, it is expected that the inertial mechanism does not lead to any bias in predicted droplet number. The same cannot be said for the evaporation and deactivation mechanisms, which tend to decrease the number of cloud droplets that are formed. Therefore using the equilibrium assumption in the presence of these two mechanisms will tend to overestimate the droplet number.

In summary, if kinetic limitations affect mainly larger particles (through the inertial mechanism), the equilibrium assumption should not induce a large error in predicted droplet number. However, if kinetic effects apply mainly to the smaller particles of a distribution, not only can the equilibrium assumption yield large error in predicted droplet number, but the droplet number will be sensitive to fluctuations in parcel supersaturation. Any factor that can influence supersaturation history (such as mode radius, number concentration, and updraft velocity) will, in turn, affect all the relevant time scales and thus the extent and type of kinetic limitations.

3. Measures of kinetic limitations

Assessing the effect of kinetic limitations on cloud droplet formation requires first the calculation of two quantities, N_{eq} and N_{kn}, the number concentrations of droplets based on equilibrium and kinetic approaches, respectively. N_{eq} is equal to the concentration of particles with critical supersaturation, S_c, less than or equal to the maximum supersaturation, S_{max}, achieved in the ascending air parcel (as calculated by the parcel model). N_{eq} is based on the assumption that the particles that can activate do so instantaneously, and is the upper limit to the number of droplets that can be formed. N_{kn} is the actual droplet concentration, and is equal to the number of particles that are larger than the activated particle with the smallest dry diameter (i.e., that has a wet radius larger than its critical value). This number contains droplets that have a critical supersaturation less than the parcel maximum supersaturation but which are not larger than their critical size. Critical parameters are calculated from classical Köhler theory (Seinfeld and Pandis, 1998).

The importance of kinetic growth limitations on droplet formation will be measured in terms

of both the activated droplet number and the cloud albedo. Based on the variation of N_{kn} and N_{eq} with cloud depth, z, one can define the total droplet ratio at any height z, $\alpha(z)$:

$$\alpha(z) = N_{kn}(z)/N_{eq}(z), \quad (1)$$

which expresses the ratio of actual droplet number to the maximum droplets attainable at a certain distance above cloud base. The droplet ratio includes both strictly activated and unactivated droplets. It is also useful, when assessing kinetic effects, to examine the portion of the droplet population that is strictly activated. For this purpose, the unactivation ratio, $\phi(z)$, defined as the fraction of droplets that are not activated, is used:

$$\phi(z) = N_{unact}(z)/N_{kn}(z), \quad (2)$$

where $N_{unact}(z)$ is the number of unactivated droplets in the distribution. For example, a $\phi(z) = 0.2$ means that 20% of the droplets are smaller than their activation diameter and thus are not strictly activated.

Profiles of $\alpha(z)$ and $\phi(z)$ can provide insight regarding the kinetic limitation mechanisms present. Fig. 2 presents a qualitative sketch of the three types of $\alpha(z)$ profiles seen in the simulations. Each type represents a case where different kinetic limitation mechanisms are active. The "type 1" profile is observed when the inertial mechanism is the only type of kinetic limitation active. In this case, $\phi(z)$ initially attains large values that decreases further up in the cloud column (not shown), and $\alpha(z)$ approaches unity with increasing z. If the evaporation mechanism is active, $\alpha(z)$ initially increases and approaches an asymptotic value less than unity; the fraction that never activates are the small particles that evaporate. This is the "type 2" profile of Fig. 2. Finally, if the deactivation mechanism is present, then the droplet ratio would initially increase, reach a maximum, and then begin to decrease as particles evaporate and deactivate.

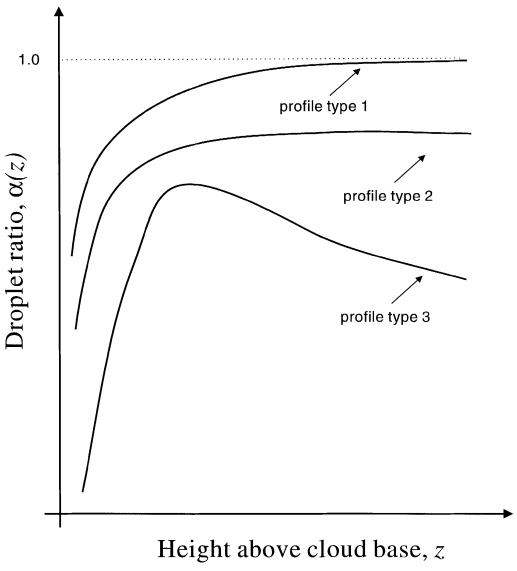

Fig. 2. Illustration of the 3 types of droplet ratio profiles seen in the simulation.

It is difficult to determine a priori when a discrepancy in cloud droplet number is important. Placed in the context of the effect on albedo, this issue becomes more straightforward; the discrepancy in droplet number can be considered significant when the albedo is biased by an amount comparable to the change induced by anthropogenic effects. Furthermore, GCMs currently implement a cloud drop number calculation for determining cloud albedo, so it is directly relevant to examine the potential error from the equilibrium activation assumption. In calculating cloud albedo, the cloud liquid water content and effective radius of the droplet distribution are used, with the assumption that the droplet distribution is narrow. Furthermore, the effect of interstitial aerosol on the liquid water content and optical properties are neglected.

4. Cloud parcel and albedo models

A cloud parcel model is the simplest tool that can be used to simulate the evolution of droplet distributions throughout a non-precipitating cloud column. These models predict a number concentration profile that starts from zero at cloud base and reaches an asymptotic value further up. In reality, droplet number and size are also affected by turbulent mixing and downdrafts, which cannot be correctly accounted for in a single parcel model. Near cloud base, where kinetic effects are strongest, droplets from upper levels tend to dry out and do not participate in the droplet distribution. Therefore, one would still expect a droplet number concentration that is zero at cloud base and quickly reaches an asymptotic value. Such distributions have been measured and predicted by

more comprehensive models (Considine and Curry, 1998), so this variation in droplet number with cloud height must be considered when calculating optical properties. Finally, existing theoretical aerosol-cloud parameterizations in GCMs are based on adiabatic cloud parcel model equations, and so estimating cloud albedo sensitivity to kinetic effects is appropriately carried out using adiabatic parcel model calculations. In order to assess the differences arising from the kinetic and thermodynamic assumptions, a droplet growth model has been incorporated within the framework of an adiabatic parcel model.

4.1. Cloud parcel model

The adiabatic cloud parcel model is based upon the parcel model described by Pruppacher and Klett (1997) and Seinfeld and Pandis (1998). Conservation of heat and moisture for a rising air parcel can be expressed as

$$\frac{dT}{dt} = -\frac{gV}{c_p} - \frac{L}{c_p}\frac{dw_v}{dt}, \tag{4}$$

$$\frac{dw_v}{dt} = -\frac{dw_c}{dt}, \tag{5}$$

where T is the temperature of the air, V is the updraft velocity, and w_v and w_c are the mixing ratios of water vapor, and liquid water in the parcel, respectively (in kg per kg air).

In (5), the condensation rate for a population of water droplets consisting of N_i droplets of radius r_i, $i = 1 \ldots n$ can be expressed as

$$\frac{dw_c}{dt} = \frac{4\pi\rho_w}{\rho_a}\sum_{i=1}^{n} N_i r_i^2 \frac{dr_i}{dt}, \tag{6}$$

where the particle growth rate is determined from,

$$\frac{dr_i}{dt} = \frac{G}{r_i}(S - S_{eq}) \tag{7}$$

with G given by

$$G = \frac{1}{\dfrac{\rho_w RT}{p_v^* D_v' M_w} + \dfrac{L\rho_w[(LM_w/RT) - 1]}{k_a' T}}. \tag{8}$$

The supersaturation S is given by $w_v/w_v^* - 1$. By integration of the supersaturation balance equation,

$$\frac{dS}{dt} = \frac{1}{w_v^*}\left[\frac{dw_v}{dt} - (S+1)\left(\frac{\partial w_v^*}{\partial T}\frac{dT}{dt} - \frac{\partial w_v^*}{\partial p_a}\rho_a g V\right)\right], \tag{9}$$

and the equilibrium supersaturation S_{eq} is given by Köhler theory:

$$S_{eq} = \exp\left(\frac{2M_w\sigma_w}{RT\rho_w r_i} - \frac{3n_s M_w v}{4\pi\rho_w(r_i^3 - r_{dry,i}^3)}\right) - 1. \tag{10}$$

Here we have used the hydrostatic relation to relate changes in atmospheric pressure to vertical velocity in (9). D_v' in (8) is the diffusivity of water vapor in air, modified for non-continuum effects,

$$D_v' = \frac{D_v}{1 + \dfrac{D_v}{a_c r}\sqrt{\dfrac{2\pi M_w}{RT}}}, \tag{11}$$

where $a_c = 1.0$ is the condensation coefficient. k_a' in (8) is the thermal conductivity of air modified for non-continuum effects,

$$k_a' = \frac{k_a}{1 + \dfrac{k_a}{a_T r\rho c_p}\sqrt{\dfrac{2\pi M_a}{RT}}}, \tag{12}$$

where $a_T = 0.96$ is the thermal accommodation coefficient, and n_s in (10) is the number of moles of solute per particle,

$$n_s = \frac{4\rho_p \varepsilon \pi d_i^3}{3M_s}, \tag{13}$$

where d_i is the dry particle diameter, and

$$\rho_p = [(1-\varepsilon)/\rho_u + \varepsilon/\rho_s]^{-1} \tag{14}$$

is the mean particle density. Surface tension σ_w is expressed (J m^{-2}) as a function of the parcel temperature T (Seinfeld and Pandis, 1998). $\sigma_w = 0.0761 - 1.55 \times 10^{-4}$ (T-273). Other symbols are defined in Section 10. Eqs. (4)–(9) constitute a closed system of ordinary differential equations that are solved numerically using the LSODE solver of Hindmarsh (1983).

4.2. Cloud albedo

Cloud albedo, R_c, is calculated based on the two-stream approximation of a non-absorbing, horizontally homogeneous cloud (Lacis and Hansen, 1974),

$$R_c = \frac{\tau}{7.7 + \tau} \tag{17}$$

where τ is the cloud optical depth,

$$\tau = \int_0^H \frac{3\rho_a w_c(z)}{2\rho_w r_{eff}(z)} dz, \quad (18)$$

where $w_c(z)$ is the liquid water mixing ratio profile along the cloud column, calculated from the parcel model simulations (after transforming the Lagrangian solution into Eulerian form by setting $w_c(z) = w_c(t)$ at $t = z/V$). ρ_w is the water density, ρ_a is the air density and $r_{eff}(z)$ is the cloud droplet distribution effective radius,

$$r_{eff} = \frac{\int_0^\infty r^3 n(r)\, dr}{\int_0^\infty r^2 n(r)\, dr}, \quad (20)$$

where $n(r)$ is the droplet size distribution. These expressions yield values for cloud albedo that are of reasonable accuracy for relatively thick clouds composed of narrow distributions of large droplets (Hatzianastassiou et al., 1997).

Assuming that the interstitial aerosol has a negligible amount of liquid water, and that the droplet population is effectively monodisperse, the expression for $r_{eff}(z)$ is given by

$$r_{eff}(z) = \left(\frac{3w_c(z)}{4\pi N_i(z)\rho_w}\right)^{1/3}, \quad (21)$$

where $N_i(z)$ can be either $N_{kn}(z)$ or $N_{eq}(z)$. In the first case, the albedo calculated will be the "kinetic albedo", while the second will be the "thermodynamic albedo". The thermodynamic albedo tends to be higher than the kinetic albedo. This is because for the same amount of cloud liquid water, the number of droplets predicted is larger in the thermodynamic case, hence the effective radius according to (21) would be smaller than in the kinetic case.

The quantity used for assessing the importance of kinetic effects, in terms of cloud albedo, is the difference between thermodynamic and kinetic albedo. Because the thermodynamic albedo is larger than the kinetic (as explained before), this difference will be positive. Furthermore, since this difference depends on the cloud depth, we select the cloud depth for which this difference is maximum.

5. Simulation parameters

The importance of kinetic limitations depends on cloud thickness, updraft velocity, and aerosol characteristics. To explore the dependence on these parameters, we shall consider a range of values spanning observations of boundary layer clouds. This study does not examine all possible phenomena that influence aerosol activation behavior, such as changes in surface tension (Facchini et al., 1999), and the presence of slightly soluble substances (Laaksonen et al., 1998). For example, a decrease in surface tension (from surfactant species in the aerosol) should enhance kinetic effects, because (a) the critical radius for activation becomes larger, so particles need more time to activate, and (b) a larger fraction of the aerosol population can activate, so more particles compete for cloud water. Solution non-idealities are not considered; they do not have a significant impact since droplets dilute considerably under supersaturated conditions (Young and Warren, 1992). Finally, the effect of uncertainty in the accommodation coefficient is not examined.

5.1. Key parameters

Cloud thickness influences the transit time of air parcels rising through a cloud, and hence the time available for particle growth. Boundary layer clouds are typically 100–500 m thick, with most in the range 200–400 m (Nichols, 1984; Duynkerke et al., 1995; Frisch et al., 1995a; White et al., 1995). To explore the dependence of kinetic effects on cloud thickness, we consider values ranging from 10 to 1000 m.

Updraft velocity influences both the transit time and the maximum supersaturation in a cloud updraft. The maximum supersaturation achieved is lower in weaker updrafts, so only particles with relatively low critical supersaturations can be activated. Observed updraft velocities in boundary layer clouds vary widely, but values derived from measured vertical velocity variance are typically 30–50 cm s^{-1} (Nichols, 1984; Duynkerke et al., 1995; Frisch et al., 1995b). We explore the dependence on updraft by considering updraft velocities of 10, 30, 100, and 300 cm s^{-1}.

5.2. Aerosol characteristics

The dependence of kinetic effects on aerosol number concentration and mean radius will be explored by considering a variety of aerosol size distributions. We consider idealized size distributions in which the number concentration and

mean radius are prescribed in order to clearly sort out the physics involved. We then consider size distributions that more closely approximate ambient distributions.

Size distributions are of the single or multiple log-normal form,

$$\frac{\mathrm{d}n(r)}{\mathrm{d}\ln r} = \sum_{i=1}^{n_\mathrm{m}} \frac{N_i}{\sqrt{2\pi}\ln\sigma_i} \exp\left[-\frac{\ln^2(r/r_{\mathrm{g},i})}{2\ln^2\sigma_i}\right], \qquad (22)$$

where N_i is the aerosol number concentration, $r_{\mathrm{g},i}$ the number mode radius, σ_i is the geometric standard deviation for mode i, and n_m is the number of modes in the distribution. For single modes we consider a single value for $\sigma = 2$, but a wide range in number concentration (100–3000 cm^{-3}) and mode radius (0.02–0.1 μm). The range in mode radius and number concentration is appropriate for accumulation mode particles, which comprise most CCN. For multiple modes we have selected four of Whitby's (1978) trimodal representations, namely the marine, clean continental, average background, and urban aerosol. The parameters of these four distributions are listed in Table 1. The size distributions refer to dry size, while the chemical composition of the aerosol is assumed pure ammonium sulfate.

In all kinetic simulations, particles are assumed initially to be in equilibrium with a relative humidity of 98%. For the idealized size distributions, we consider 200 size bins spaced equally in log radius. Using a size range between about $D_{\mathrm{p,g}}/10\sigma$ and $10\sigma D_{\mathrm{p,g}}$ covers total particle number to within 10^{-7}%. The simulations exhibit little sensitivity with respect to initial relative humidity concentrations and denser discretization.

6. Effect of kinetic limitations on cloud droplet number

We first explore the parametric dependence of kinetic limitations using the single log-normal size distributions. We then consider various multimode log-normal distributions that resemble ambient aerosol.

6.1. Single log-normal size distributions

From the simulations we calculate the $\alpha(z)$ and $\phi(z)$ profiles. The results of these simulations are summarized in Table 2, which gives the characteristics of these ratios for all the mode radii, number concentrations, and updrafts examined. As expected, the droplet ratio (for constant mode radius and number concentration) in most cases approaches an asymptotic value for large cloud depths. Kinetic effects become more apparent as updraft velocity decreases and aerosol concentrations increase. For a mode radius of 0.03 μm, the droplet number is reduced by 40% for an updraft velocity of 10 $\mathrm{cm\,s}^{-1}$ and an aerosol number concentration of 3000 cm^{-3}. In this particular example, the unactivation ratio $\phi(z)$ is close to zero. This means that most (more than 95%) of the cloud drops are activated. In addition, the droplet ratio profile is "type 3", so both evaporation and deactivation mechanisms are present.

The dependence of kinetic effects on N_i is further pronounced as mode radius increases. For example, the droplet ratio for an aerosol number concentration of 3000 cm^{-3} and a mode radius of 0.1 μm can be close to zero for a large portion of the cloud, because the time required for growth is very large for weak updrafts (this is also seen in $\phi(z)$, which ranges between 1.0 and 0.083). In this particular case, the profile $\alpha(z)$ is "type 2", so the evaporation mechanism is present. The fact that $\alpha(z)$ is maximum at 700 m above cloud base indicates that kinetic effects are very strong. This is not surprising, given the mode radius and concentration of particles. As updraft velocity increases, supersaturation, being the driving force for particle growth, also increases and activates particles lower

Table 1. *Aerosol distribution parameters ($r_{g,i}$ in μm, N_i in cm^{-3}) (Whitby et al., 1978)*

	Nuclei mode		Accumulation mode		Coarse mode				
Aerosol type	$r_{\mathrm{g},1}$	σ_1	N_1	$r_{\mathrm{g},2}$	σ_2	N_2	$r_{\mathrm{g},3}$	σ_3	N_3
marine	0.005	1.6	340	0.035	2.0	60	0.31	2.7	3.1
clean continental	0.008	1.6	1000	0.034	2.1	800	0.46	2.2	0.72
average background	0.008	1.7	6400	0.038	2.0	2300	0.51	2.16	3.2
urban	0.007	1.8	106000	0.027	2.16	32000	0.43	2.21	5.4

Table 2. *Summary of single lognormal aerosol distribution simulations; α_{max} is the maximum value of $\alpha(z)$, encountered at $z_{\alpha_{max}}$ above cloud base*

$r_{g,i}$ (μm)	N_i (cm^{-3})	V ($m\ s^{-1}$)	Droplet profile type	α_{max}	$z_{a_{max}}$ (m)	α (1000 m)	ϕ (20 m)	ϕ (1000 m)
0.03	100	0.1	1	1.000	10	1.000	0.002	0.000
0.03	100	0.3	1	1.000	20	1.000	0.006	0.042
0.03	100	1.0	1	1.000	20	1.000	0.024	0.026
0.03	100	3.0	1	1.000	20	1.000	0.095	0.012
0.03	300	0.1	2	0.931	10	0.931	0.005	0.000
0.03	300	0.3	3	1.000	10	0.948	0.008	0.000
0.03	300	1.0	1	1.000	20	1.000	0.028	0.000
0.03	300	3.0	1	1.000	20	1.000	0.095	0.020
0.03	1000	0.1	3	0.918	10	0.768	0.014	0.000
0.03	1000	0.3	3	1.000	10	0.936	0.019	0.000
0.03	1000	1.0	2	0.956	10	0.956	0.037	0.000
0.03	1000	3.0	1	1.000	20	1.000	0.103	0.029
0.03	3000	0.1	3	0.815	10	0.589	0.052	0.000
0.03	3000	0.3	3	0.922	10	0.713	0.050	0.000
0.03	3000	1.0	3	0.944	10	0.889	0.066	0.000
0.03	3000	3.0	3	1.000	20	0.961	0.141	0.001
0.05	100	0.1	1	1.000	10	1.000	0.019	0.042
0.05	100	0.3	2	0.974	10	0.974	0.032	0.000
0.05	100	1.0	1	1.000	20	1.000	0.092	0.013
0.05	100	3.0	1	1.000	20	1.000	0.231	0.004
0.05	1000	0.1	3	0.857	10	0.668	0.159	0.001
0.05	1000	0.3	3	0.948	10	0.847	0.154	0.001
0.05	1000	1.0	2	0.970	20	0.970	0.177	0.002
0.05	1000	3.0	1	0.985	20	0.985	0.323	0.003
0.10	100	0.1	3	0.974	10	0.948	0.206	0.005
0.10	100	0.3	1	1.000	10	1.000	0.244	0.006
0.10	100	1.0	1	1.000	20	1.000	0.386	0.008
0.10	100	3.0	1	1.000	30	1.000	0.586	0.009
0.10	300	0.1	3	0.908	20	0.774	1.000	0.011
0.10	300	0.3	3	0.954	20	0.929	0.414	0.014
0.10	300	1.0	1	1.000	20	1.000	0.422	0.024
0.10	300	3.0	1	0.998	30	0.998	0.671	0.018
0.10	1000	0.1	3	0.925	200	0.785	1.000	0.034
0.10	1000	0.3	3	0.950	70	0.804	1.000	0.033
0.10	1000	1.0	3	0.979	20	0.933	1.000	0.036
0.10	1000	3.0	1	1.000	20	0.994	0.755	0.040
0.10	3000	0.1	2	0.902	700	0.902	1.000	0.133
0.10	3000	0.3	3	0.925	500	0.853	1.000	0.102
0.10	3000	1.0	3	0.952	200	0.857	1.000	0.086
0.10	3000	3.0	3	0.979	50	0.933	1.000	0.083

in the cloud. The dependence on cloud thickness is also stronger for a mode radius of 0.1 μm than for 0.03 μm because (a) maximum supersaturation is achieved further up from cloud base, and, (b) the larger particles respond more slowly to variations in supersaturation. The deactivation mechanism is responsible for decreasing the droplet ratio for low updrafts and high number concentrations ($>$ 300 cm^{-3}). Another striking feature, as evidenced by $\phi(z)$, is that the inertial mechanism is negligible for particles of smaller modal diameter; in the larger size distributions, roughly half of the particles are not activated during the first 50–100 m of the cloud. Despite the difference in modal size, the fraction of small particles that fail to activate is roughly the same at large cloud depths.

The simulations indicate that a large mode radius tends to accentuate kinetic effects. By exam-

ining $\alpha(z)$ and $\phi(z)$ as a function of mode radius for a number concentration of 100 cm^{-3}, we can see that evaporation and deactivation effects are negligible for all mode radii; most droplet ratio profiles are of type 1. Inertial effects (as shown by the value of $\phi(z)$ at 20 m) become increasingly important as mode radius increases. On the other hand, $\alpha(z)$ never drops below 0.95. This is an important point: for low concentration of particles, kinetic effects that influence droplet number are negligible regardless of particle diameter. The inertial mechanism is the only type of limitation experienced by these particles.

Kinetic effects are more prominent when the number concentration increases to 1000 cm^{-3}. When the concentration of particles is this high, profile types indicate that the deactivation and evaporation mechanisms are much more prominent than for a particle concentration of 100 cm^{-3}. This suggests that these kinetic limitation mechanisms are present primarily at high number concentrations.

6.2. *Trimodal log-normal size distributions*

From the previous section, it is clear that kinetic limitations on droplet formation are important for high number concentrations, and large mean particle size can further enhance these effects. Although one can imagine combinations of number concentration and mean particle size that would yield significant kinetic limitations, such combinations may not be realistic. High particle concentrations are normally associated with small particle sizes, and vice versa. An assessment of the importance of kinetic limitations on ambient droplet formation should therefore consider size distributions that represent ambient aerosol. In doing so, we examine the trimodal log-normal fits to measured size distributions for a variety of aerosol types in Table 1.

Although the number concentration for the nuclei mode can be quite large, the particles are so small that the supersaturation necessary for activating them is never encountered within a cloud. Furthermore, the mean particle size of the coarse mode is large enough for significant kinetic effects, but the number concentrations are usually too small to have a significant impact on droplet number. Thus, the distribution characteristics of the accumulation mode is expected to determine the kinetic effects of the aerosol types in Table 1.

Fig. 3 shows $\alpha(z)$ and $\phi(z)$ as a function of updraft velocity and cloud thickness for the aerosol types shown in Table 1. Simulations reveal that kinetic effects for the marine aerosol are negligible regardless of updraft velocity and cloud thickness. This is not surprising, given that the number concentration of the accumulation mode, 60 cm^{-3}, is too low for kinetic effects to be important.

The accumulation mode number concentration for the clean continental aerosol is much higher, 800 cm^{-3}, so kinetic effects become evident at weak updraft velocities: $\alpha(z)$ is always below 0.85 for $V = 10$ cm s^{-1}, and 0.95 for $V = 30$ cm s^{-1}. Results for the clean continental aerosol are comparable to those illustrated in Table 2 for a number mode radius of 0.03 μm and a number concentration of 1000 cm^{-3}, but with kinetic effects being somewhat weaker because of the lower number concentration. The ratio $\phi(z)$, however, is low and the droplet ratio approaches an asymptotic value, so the aerosol is subject to the evaporation mechanism, as some of the particles fail to activate in the initial stages of cloud formation.

Kinetic limitations on droplet formation are quite important for the average background aerosol, which has an accumulation mode number concentration of 2300 cm^{-3}. The droplet ratio is a little over 0.8 for a 30 cm s^{-1} updraft, which is consistent with the single log-normal size distribution with the same number concentration. Although there are strong inertial effects in the coarse mode, its contribution to the total droplet number concentration is rather small. Because of this, $\phi(z)$ is low, less than 0.1 for cloud depths larger than 20 m, indicating that most of the droplets are strictly activated. For weak updrafts, because of the high concentration of accumulation mode particles, deactivation plays a significant role and reduces the droplet number by 20%. Overall, the aerosol seems to be subject to both deactivation and evaporation mechanisms, the degree to which depends on the updraft velocity.

With an accumulation mode number concentration of 32,000 cm^{-3}, one might expect substantial kinetic effects for the urban aerosol, and indeed this is the case. In fact, kinetic effects are so strong, that $\alpha(z)$ is zero until 70 m above cloud base. The activation ratio never exceeds 0.8, even for the

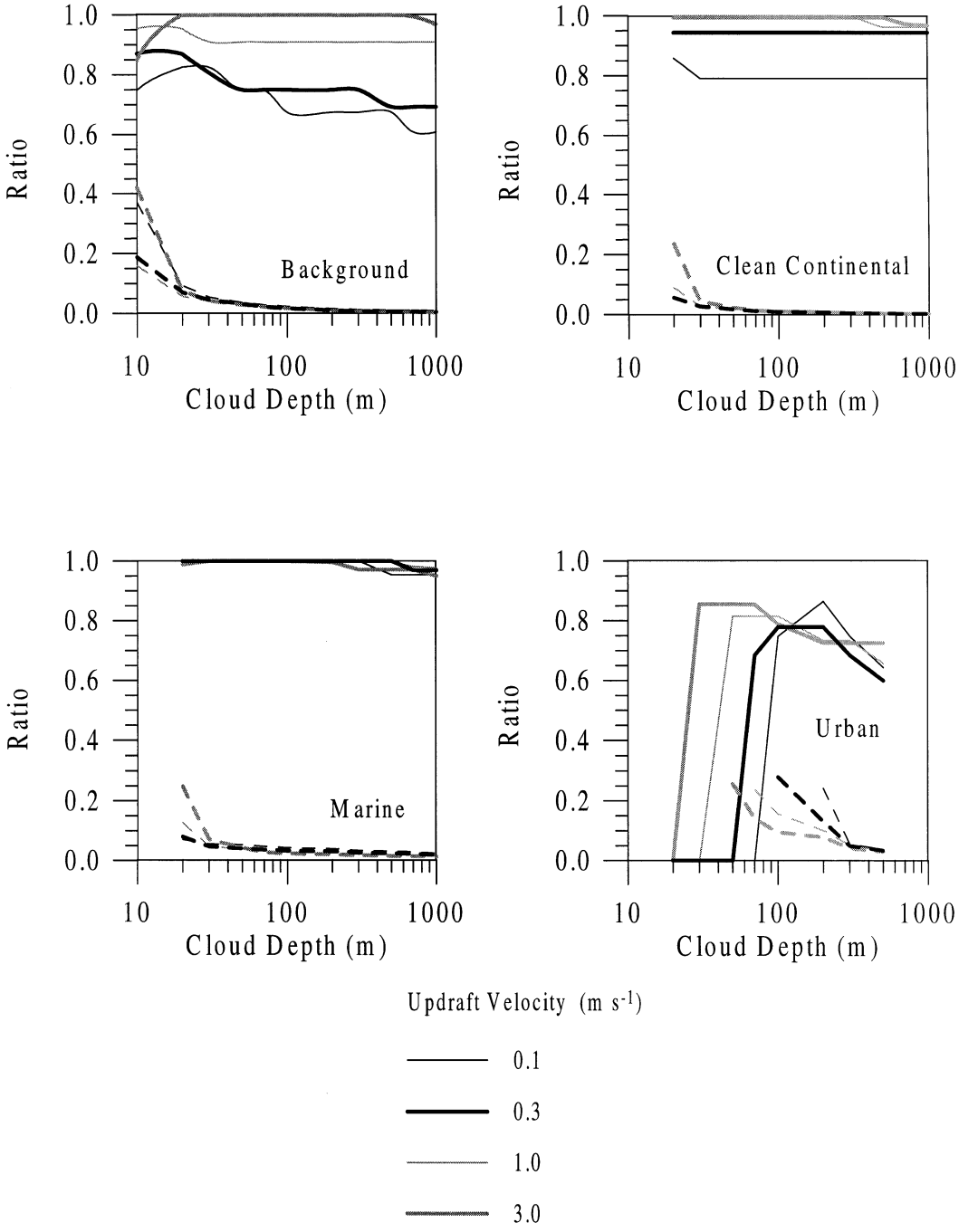

Fig. 3. Droplet and unactivation ratios as a function of updraft velocity and cloud thickness for the background, clean continental, marine, and urban distributions of Table 1. Solid lines represent the droplet ratio $\alpha(z)$, while dashed lines represent the unactivation ratio $\phi(z)$.

strongest updrafts. The latter indicates that many particles fail to activate as the supersaturation decreases following the maximum supersaturation in all updraft cases examined. Inertial effects are also significant; even for clouds of 200 m thickness, $\phi(z)$ is above 0.2. Finally, deactivation is also very strong since the decrease in $\alpha(z)$ after the maximum is about 20%.

7. Effect of kinetic limitations on cloud albedo

For very thin clouds (of the order of 10 m), the optical depth is small, so the albedo difference itself is small. As the cloud depth increases, so does optical depth. This initially leads to an increase in the albedo difference; after a certain point, the optical depth is so large, that the albedo difference begins to decrease. The point of maximum difference between thermodynamic and kinetic albedo is used for evaluating kinetic effects. A climatically important kinetic effect would be considered for a difference between kinetic and thermodynamic albedo larger than about 0.005; this albedo change, if relevant globally, could yield an uncertainty in radiative forcing comparable to that estimated for anthropogenic indirect aerosol radiative forcing (Facchini et al., 1999). It should also be noted that the maximum albedo difference in the simulations (both single mode and trimodal distributions) was encountered in the first 300 m of the cloud. As expected, increasing the kinetic effects for constant updraft tends to shift the locus of the maximum higher up in the cloud.

7.1. *Single log-normal size distributions*

Since the difference between thermodynamic and kinetic cloud albedo depends on the difference in cloud droplet number, it is expected that the largest difference would be seen for high number concentrations. The discrepancy is also expected to be enhanced if the distribution has a large modal radius. This can be seen in the two top panels of Fig. 4, which shows the maximum albedo difference, as a function of number concentration, for two modal radii. For a number mode radius of 0.03 μm (top left panel), there is large sensitivity of kinetic effects on albedo to number concentration. For low concentrations ($100\,cm^{-3}$), kinetic limitations are not strong enough to yield a significant difference in cloud albedo; this difference becomes very large however, close to 0.05, when the concentration is around $3000\,cm^{-3}$. For a number mode radius of 0.1 μm (top right panel), these effects are enhanced considerably and the albedo difference approaches 0.7 for the lowest updraft and highest number concentrations. The cases where albedo difference is below 0.005 seem to be the same for both mode radius cases, when the number concentration is below $300\,cm^{-3}$.

The above statements are further supported by the two bottom panels of Fig. 4. These show the maximum albedo difference as a function of mode radius, for two number concentrations. Regardless of modal radius, when the concentration is $100\,cm^{-3}$ (bottom left panel) the albedo difference is insignificant. However, when the concentration becomes $1000\,cm^{-3}$, kinetic effects are almost always significant. When the albedo difference is around 0.1, the effect of mode radius seems to be small.

By comparing Fig. 4 with Table 2, we observe a consistent trend; the maximum albedo difference tends to exceed the 0.005 value whenever the droplet ratio consistently (that is, for all cloud depths) is below 0.9. This is an important point, since it provides a quantitative measure for when the bias in droplet number becomes important.

7.2. *Trimodal log-normal size distributions*

Fig. 5 shows the maximum difference in cloud albedo between the thermodynamic and kinetic activation models, for the four log-normal distributions of Table 1. Albedo differences are shown for both the total number concentration in Table 1 and twice these values. The urban aerosol distribution exhibits the largest difference in albedo, which is expected, given that it is the distribution with the largest kinetic limitation effects in droplet number. Of the other aerosol classes, the largest sensitivity is experienced by the clean continental aerosol, where a doubling in concentration leads to a fivefold increase in albedo difference (at the highest updraft velocities). As in Subsection 7.1, kinetic limitations become important for cloud albedo whenever $\alpha(z)$ is consistently below 0.9.

8. Summary and conclusions

There are three mechanisms that lead to kinetic limitations on cloud droplet formation. The first,

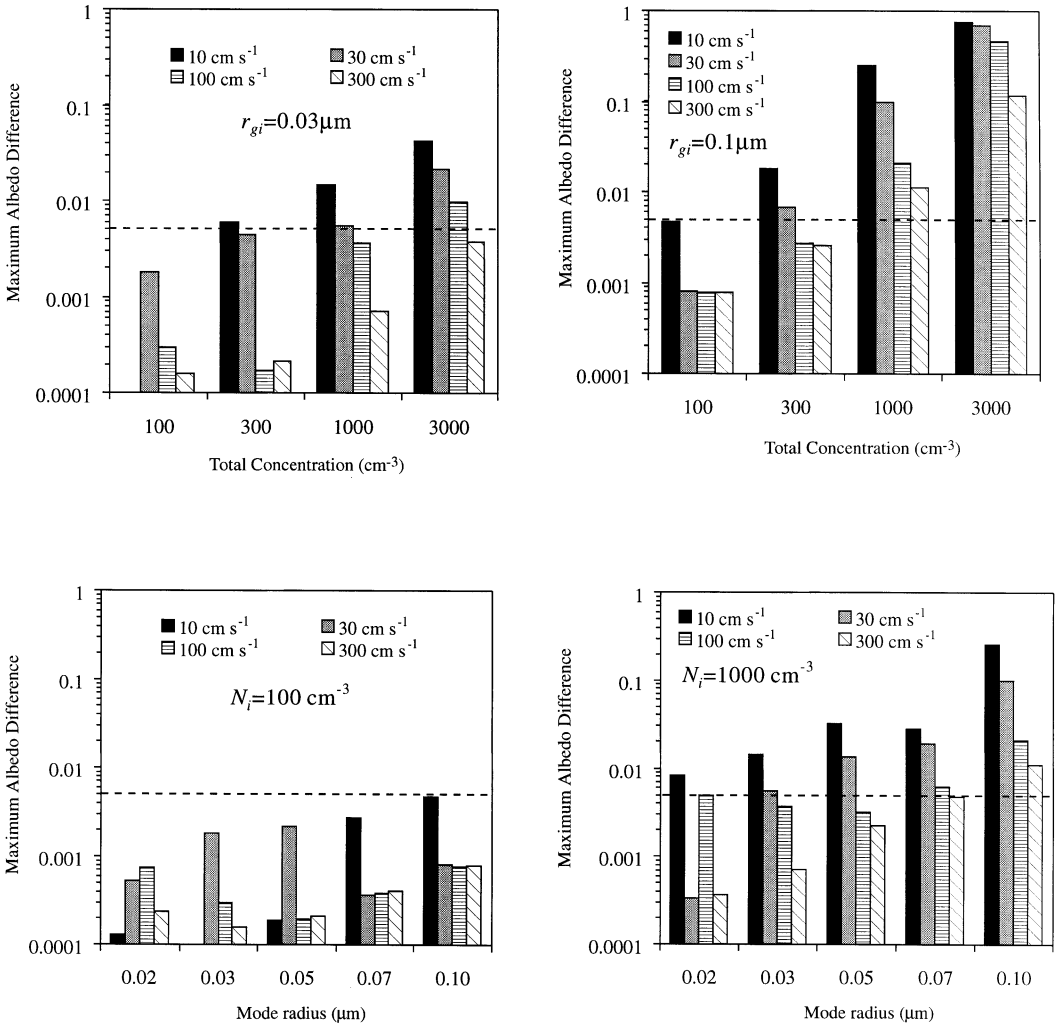

Fig. 4. Maximum difference between thermodynamic and kinetic cloud albedo. The single model log-normal distribution is used with (a) number mode radius 0.03 μm, (b) number mode radius 0.1 μm, (c) number concentration of 100 cm^{-3}, and (d) number concentration of 1000 cm^{-3}.

identified by Chuang et al. (1997), and termed the *inertial mechanism*, arises when particles with critical supersaturation less than a threshold value do not have time to grow larger than their critical size and thus do not activate. In the second *deactivation mechanism*, activated droplets evaporate to form interstitial aerosol when the parcel supersaturation drops below the droplet equilibrium saturation ratio. In the third mechanism, the *evaporation mechanism*, particles that could potentially activate (because their critical supersaturation is low enough) evaporate to form interstitial aerosol because the time they are exposed to high supersaturation is not sufficient to reach their critical radius. Large particles, which are subject to the inertial mechanism, are also large enough to be considered cloud droplets even when they are not strictly activated. Particles, however, that are subject to the deactivation and evaporation mechanisms become much smaller than activated drops and hence should not be considered cloud droplets. Thus, if deactivation

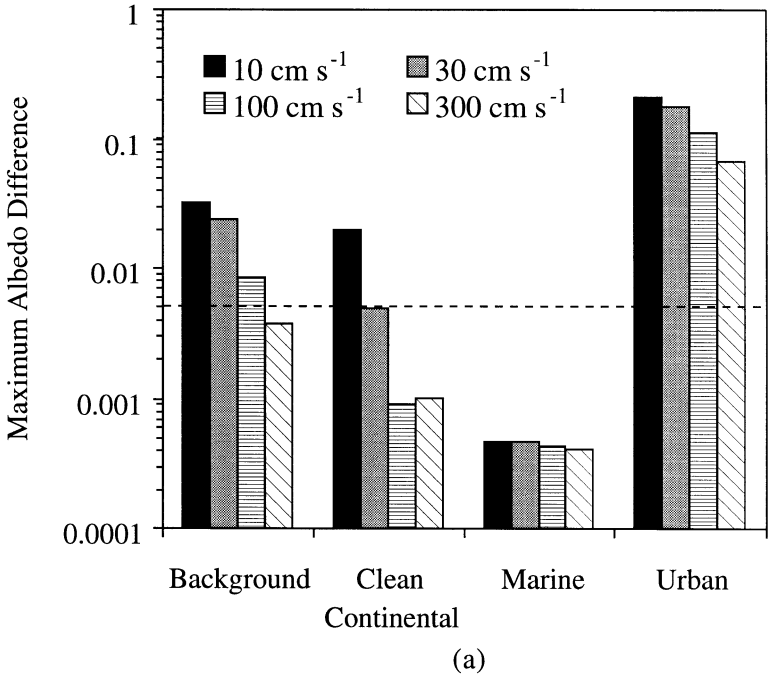

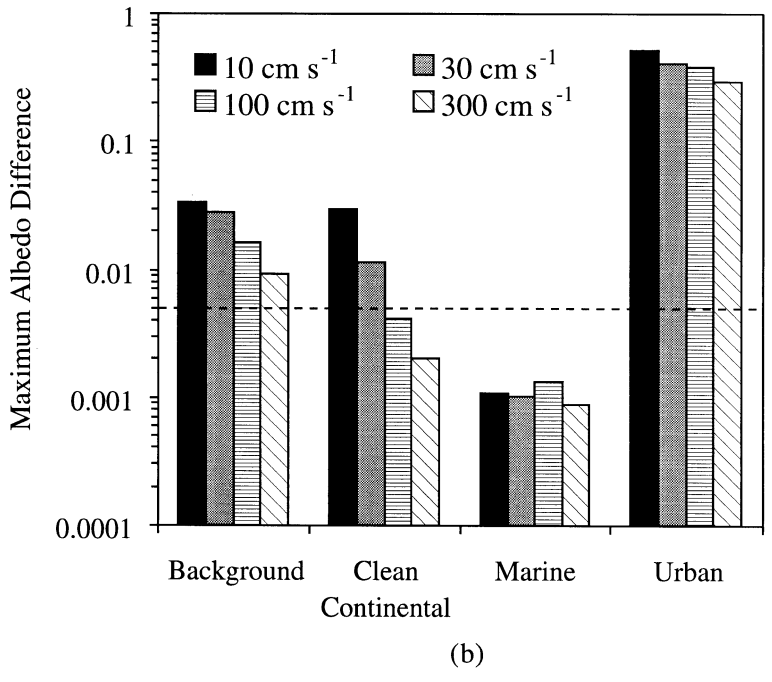

Fig. 5. Maximum difference between thermodynamic and kinetic cloud albedo. The aerosol distributions in Table 1 are used with (a) given number concentrations, and (d) doubled number concentrations.

and evaporation significantly reduce the droplet number concentration, these processes should be accounted for in parameterizations of the activation process. The inertial mechanism, although a type of kinetic limitation, does not generate a discrepancy in cloud droplet number. Most of the discrepancy is a result of the smaller particles that fail to activate, through the two other mechanisms identified. This also implies that for cases which kinetic effects are significant, the droplet number is quite sensitive to fluctuations in supersaturation.

In terms of number of cloud droplets, the conditions most likely to yield considerable kinetic effects are those of high aerosol number concentrations. Weak updrafts and large mode radius tend to enhance kinetic effects. We have also investigated a variety of aerosol types to determine those subject to important kinetic effects under a variety of cloud formation conditions. We have found that anthropogenically-influenced aerosol is strongly affected by kinetic growth limitations, but relatively pristine marine aerosols are not. We have found that for most aerosols the percentage errors from neglecting kinetic effects are larger for weak updrafts than for strong updrafts, even though the residence time of air parcels in clouds is shorter for strong updrafts. However, absolute errors in droplet number are often largest for moderate updrafts because aerosol activation is inefficient for weak updrafts, and kinetic limitations are smaller for strong updrafts.

The conditions most likely to yield considerable differences in cloud albedo are similar to those for droplet number, i.e., weak updrafts, large mode radius, and high aerosol concentrations. Simulations indicate that the maximum albedo difference is less than 0.005 for marine aerosol (where kinetic limitations in cloud droplet number are also not significant). Albedo differences can, however, exceed 0.1 for urban aerosol.

By comparing the droplet ratio and albedo difference plots, it can be seen that kinetic effects become important whenever the droplet ratio is consistently below 0.9. Of the 3 kinetic limitation mechanisms, the evaporation and deactivation mechanisms can influence droplet number concentrations. However, the deactivation mechanism does not affect aerosol throughout the cloud and always appears together with the evaporation mechanism. So, it is believed that conditions that are conducive towards the appearance of the evaporation mechanism can lead to substantial kinetic effects. As a consequence, kinetic limitations are not expected overall to be climatically significant, but can have a noticeable local impact.

Existing parameterizations of aerosol activation in GCMs do not usually account for kinetic limitations. Because closed-form solutions of the activation process are not available, parameterizations can be fit to kinetic simulations. Future parameterizations should therefore be matched to kinetic simulations that extend beyond the point of maximum supersaturation, classify activated particles on the basis of their size rather than their critical supersaturation, and also account for fluctuations that may occur in cloud supersaturation.

9. Acknowledgements

This work was supported at PNNL by the NASA Earth Science Enterprise under contract NAS5-98072 and by the US Department of Energy Atmospheric Radiation Measurement Program, which is part of the DOE Biological and Environmental Research Program. PNNL is operated for the DOE by Battelle Memorial Institute under contract DE-AC06-76RLO 1830. This work as supported at the California Institute of Technology by the Office of Naval Research.

10. Appendix

Notation

a_c	condensation coefficient
a_T	thermal accommodation coefficient
c_p	specific heat of dry air at constant pressure
r_{dry}	particle dry radius
D_v	water vapor diffusivity in air
D'_v	water vapor diffusivity in air, corrected for non-continuum effects
g	acceleration of gravity
G	particle growth parameter, as given by (8)
H	cloud thickness
k_a	thermal conductivity of air
k'_a	thermal conductivity of air, corrected for non-continuum effects
L	latent heat of condensation of water

M_a	molecular weight of dry air
M_s	molecular weight of the solute
M_w	molecular weight of water
$n(r)$	number size distribution
n_m	number of modes in idealized log-normal distributions
n_s	number of moles of solute per particle
N	aerosol number concentration
N_{eq}	number concentration of particles with S_c smaller than or equal to S_{max}
N_{kn}	number concentration of particles with dry radius larger than that of the smallest activated particle
N_{unact}	number concentration of large unactivated particles (with dry radius larger than that of the smallest activated particle, but with a wet radius less than the critical size)
p_a	air pressure
p_v^*	saturation vapor pressure of water
r	particle wet radius
$r_{g,i}$	number mode radius of log-normal size distribution
r_{eff}	size distribution effective radius
R	universal gas constant
R_c	cloud albedo
S	supersaturation
S_c	critical supersaturation for activating according to Köhler theory
S_{eq}	supersaturation in equilibrium with particle size
S_{max}	maximum supersaturation in a cloud parcel
t	time
T	temperature of air parcel
V	parcel updraft velocity
w_v	water vapor mixing ratio in air parcel
w_c	cloud liquid water mixing ratio
w_v^*	p_v^*/p_a saturation mixing ratio of water
z	cloud depth as measured from cloud base (or where $S = 0\%$)
α	droplet ratio N_{kn}/N_{eq}
ε	mass fraction of soluble material in the dry particle
v	number of ions the solute dissociates into in solution
ρ_a	density of air
ρ_w	density of water
ρ_p	mean density of particle
ρ_s	density of soluble component of particle
ρ_u	density of insoluble component of particle
σ	geometric standard deviation of the aerosol size distribution
σ_w	water surface tension
τ	optical depth
ϕ	unactivation ratio N_{unact}/N_{kn}

REFERENCES

Abdul-Razzak, H., Ghan, S. J. and Rivera-Carpio, C. 1998. A parameterization of aerosol activation. Part I: Single aerosol type. *J. Geophys. Res.* **103**, 6123–6132.

Chuang, P. Y., Charlson, R. J. and Seinfeld, J. H. 1997. Kinetic limitations on droplet formation in clouds. *Nature* **390**, 594–596.

Considine, G. and Curry, J. A. 1998. Effects of entrainment and droplet sedimentation on the microphysical structure of stratus and stratocumulus clouds. *Q. J. R. Meteorol. Soc.* **124**, 123–150.

Duynkerke, P. G., Zhang, H. Q. and Jonker, P. J. 1995. Microphysical and turbulent structure of nocturnal stratocumulus as observed during ASTEX. *J. Atmos. Sci.* **52**, 2763–2777.

Facchini, M. C., Mircea, M., Fuzzi, S. and Charlson, R. J. 1999a. Cloud albedo enhancement by surface-active organic solutes in growing droplets, *Nature* **401**, 257–259.

Frisch, A. S., Fairall, C. W. and Snider, J. B. 1995a. Measurement of stratus cloud and drizzle parameters in ASTEX with a K_α-band doppler radar and a microwave receiver. *J. Atmos. Sci.* **52**, 2788–2799.

Frisch, A. S., Lenschow, D. H., Fairall, C. W., Schubert, W. H. and Gibson, J. S. 1995b. Doppler radar measurements of turbulence in marine stratiform cloud during ASTEX. *J. Atmos. Sci.* **52**, 2800–2808.

Ghan, S. J., Chuang, C. C. and Penner, J. E. 1993. A parameterization of cloud droplet nucleation. Part I: Single aerosol species. *Atmos. Res.* **30**, 197–222.

Hatzianastassiou, N., Wobrock, W. and Flossman, A. I. 1997. The role of droplet spectra for cloud radiative properties. *Q. J. R. Meteorol. Soc.* **123**, 2215–2230.

Hindmarsh, A. C. 1983. ODEPACK: a systemetized collection of ODE solvers. *Scientific Computing*, edited by R. S. Stepleman et al., pp. 55–64, North-Holland, New York.

Laaksonen, A., Korhonen, P., Kulmala, M. and Charlson, R. J. 1998. Modification of the Köhler equation to include soluble trace gases and slightly soluble substances. *J. Atmos. Sci.* **55**, 853–862.

Lacis, A. A. and Hansen, J. E. 1974. A parameterization of the absorption of solar radiation in the Earth's atmosphere, *J. Atmos. Sci.* **31**, 118–133.

Liu, X. H. and Wang, M. K. 1996. A parameterization

of the efficiency of nucleation scavenging of aerosol particles and some related physicochemical factors. *Atmos. Env.* **30**, 2335–2341.

Nichols, S. 1984. The dynamics of stratocumulus: aircraft observations and comparisons with a mixed layer model. *Quart J. R. Met. Soc.* **110**, 783–820.

Pandis, S. P., Seinfeld, J. H. and Pilinis, C. 1990. The smog-fog-smog cycle and acid deposition. *J. Geophys. Res.* **95**, 18,489–18,500.

Pruppacher, H. R. and Klett, J. D. 1997. *Microphysics of clouds and precipitation.* Kluwer, Dordrecht.

Seinfeld, J. H. and Pandis, S. N. 1998. *Atmospheric chemistry and physics.* John Wiley, New York.

Whitby, K. T. 1978. The physical characteristics of sulfur aerosols. *Atmos. Environ.* **12**, 135–159.

White, A. B., Fairall, C. W. and Snider, J. B. 1995. Surface-based remote sensing of marine boundary-layer cloud properties. *J. Atmos. Sci.* **52**, 2827–2838.

Young, K. C. and Warren, A. J. 1992. A reexamination of the derivation of the equilibrium supersaturation curve for soluble particles. *J. Atmos. Sci.* **49**, 1138–1143.